Ки&М

ANALYSIS AND MODELING OF COMPLEX LIVING SYSTEMS

UDC: ???.??

The dynamics of monkeypox transmission with an optimal vaccination strategy through a mathematical modelling approach

M. Zevika[1,2,a], A. Triska[3,b], J. W. Puspita[1,4,c]

[1]Department of Mathematics, Institut Teknologi Bandung,
Bandung, Indonesia
[2]Research Center for Applied Zoology, National Research and Innovation Agency,
Bogor, Indonesia
[3]Department of Mathematics, Universitas Padjadjaran,
Bandung, Indonesia
[4]Mathematics Study Program of Science Faculty, Tadulako University,
Palu, Indonesia

E-mail: [a] monzevik@s.itb.ac.id, [b] a.triska@unpad.ac.id, [c] juni.wpuspita@yahoo.com

Monkeypox is a disease reemerging in 2022 which is caused by the monkeypox virus (MPV). This disease can be transmitted not only from rodents to humans, but also from humans to other humans, and even from the environment to humans. In this work, we propose a mathematical model to capture the dynamics of monkeypox transmission which involve three modes of transmission, namely, from rodents to rodents, rodents to humans, and from humans to other humans. In addition to the basic reproduction number, we investigate the stability of all equilibrium points analytically, including an implicit endemic equilibrium by applying the center manifold theorem. Moreover, the vaccination as an alternative solution to eradicate the monkeypox transmission is discussed and solved as an optimal control problem. The results of this study show that the transmission of monkeypox is directly affected by the internal infection rates of each population, i. e., the infection rate of the susceptible human by an infected human and the infection rate of the susceptible rodent by an infected rodent. Furthermore, the external infection rates, i. e., the infection rate of the susceptible human by an infected rodent also affects the transmission of monkeypox although it does not affect the basic reproduction number directly.

Keywords: SEIR-SEIR model, monkeypox, vaccination, optimal control, forward bifurcation

Introduction

After more than two years the global economy and healthcare have been impacted by Coronavirus disease (Covid-19), now it seems to enter an endemic stage. Unfortunately, according to prediction of medical research that reported in [Kumar et al., 2022; Bryer, Freeman, Rosenbach, 2022; Velavan, Meyer, 2022], we will likely be facing a second new viral outbreak of a zoonotic infection with the etiological agent, the monkeypox virus (MPV). The MPV causes a disease which is known as monkeypox [McCollum, Damon, 2014]. Monkeypox is classified as a zoonotic infection which means that it can spread from animals to humans. It can also spread from a human to other humans and from the environment to humans [WHO].

This disease was first discovered in 1958 in Copenhagen [Kampf, 2022]. However, most cases of human monkeypox which have been reported from time to time are observed in West Africa and Central Africa that are endemic regions for this virus [Bhattacharya, Dhama, Chakraborty, 2022]. But this virus spread through international travelers from time to time [Reynolds et al., 2019] which may trigger a new outbreak in many countries. During May and June 2003, the first cluster of human monkeypox cases in the United States was reported [Meo, Jawaid, 2022]. Most patients with this febrile vesicular rash illness presumably acquired the infection from prairie dogs [Guarner et al., 2004]. Furthermore, monkeypox became an outbreak in the Democratic Republic of Congo (DRC) in 2013, which was reported from 26 health districts which contain 512 health zones [Nolen et al., 2016]. In most cases, symptoms of monkeypox go away on their own within a few weeks. However, in some people, an infection can lead to medical complications and even death [Sah et al., 2022]. Based on what we know from previous monkeypox outbreaks, new-born babies, children and people with underlying immune deficiencies may be at higher risk of more serious symptoms and death from monkeypox [WHO].

Monkeypox could spread from an infected animal, such as antelope, gazelle, tree squirrel, or terrestrial rodent, even from a primate, to human when there is physical contact between them [Bell, Cunningham, 2022]. Here, physical contacts itself can go through bites or scratches from those animals. People may get these physical contacts during activities such as hunting or trapping [WHO]. People can also be exposed to the virus while eating infected animals if they are not cooked thoroughly [Lai et. al., 2022]. The transmission of monkeypox from animals to humans can be avoided by reducing unprotected contact with blood or meat of sick or dead wild animals. Besides, monkeypox can also spread from an infected human to the susceptible humans through a close contact [Murphy, Ly, 2022]. Facing each other at close range while talking and breathing which produces short-range droplets or aerosols is included in a close contact among humans [Alakunle et al., 2020]. Moreover, its spread is also possible by contact of skin to skin such as touching or sexual activities. Nevertheless, the spread of monkeypox through the air is not yet well understood until now. Thus, the research on the possible mechanism of spreading it is underway [WHO].

Recently, monkeypox infection was reported again on May 18, 2022 in Canada, Spain, and Portugal with total cases of 13, 7, and 14, respectively [BBC News]. On the same day, Spain also reported their first case of MPV. Still in May, 2022, some countries in Europe confirmed their first MPV cases, i. e., Italy, Sweden, and Belgium. Next, Australia reported on two patients of MPV who had recently returned from Europe on May 20, 2022, which occurred from two different cities, namely, in Melbourne and Sydney. Back to Europe, on the same date, Netherlands, Germany, and France confirmed their first cases. Like the United Kingdom (UK), they reported other eleven cases of MPV so that there are 71 cases of MPV in total [Gov.UK]. The next day, Israel and Switzerland also confirmed their first cases. On May 23, Denmark followed by reporting their first case. On May 24, 2022, Canada announced 15 confirmed cases in Quebec, where at that time, the Czech Republic confirmed its first case. In this case, the patient participated in an international music festival in Belgium before. In late May, the United Arab Emirates confirmed its first case, namely, a 29-year-old woman who had

visited West Africa before. Next, Slovenia also confirmed its first case. Therefore, until May 2022 there have been 19 countries that reported MPV cases. In the following month, on June 3, Spain reported again an increase in the number of cases of MPV to a total of 186 [Reuters, 2022]. The spread of the recent outbreak that occurred after the first infections affected to someone who travelled from the endemic regions of Africa to North America and Europe. The characteristics of monkeypox which can be transmitted from human to human and even from animal to human make it easy to spread. However, the source of the ongoing MPV outbreak is still being confirmed [Kumar et al., 2022].

Researches on monkeypox was limited and received little attention in the past and this contributed to insufficient knowledge of its transmission mechanisms. A few studies have tried to understand the dynamics of the monkeypox transmission using a compartmental mathematical models technique. Bankuru et al. [Bankuru et al., 2020] constructed a mathematics model which consists of two populations, namely, human and host population. They assume squirrels as the primary hosts of transmission of monkeypox from animal to humans. Each population is divided into Susceptible-Exposed-Infected-Recovery (SEIR) compartments, but they consider vaccination compartment in human population. Peter et al. [Peter et al., 2022] consider a SQEIR-SEI mathematics model of monkeypox transmission without vaccination compartment of humans and recovery compartment of the host. Here, they assume rodent as the hosts of transmission of monkeypox from animal to humans. In contrast to [Bankuru et al., 2020; Peter et al., 2022], Khaloufi et al. [Khaloufi et. al., 2022] studied the spread of monkeypox which considered the transmission of this disease form human to humans only.

Moreover, Usman et al. in [Usman, Ibrahim, 2017] discussed the monkeypox model with vaccination compartment and consider the death caused by monkeypox itself. However, according to [Sah et al., 2022] the death rate caused by monkeypox is not significant so it can be ignored. In some cases, a complex model causes limitation analytical results. Thus, in the present study, we modify the model of Peter et al. [Peter et al., 2022], Bankuru et al. [Bankuru et al., 2020], and [Usman, Ibrahim, 2017] in order to complete the dynamical analysis for each equilibrium point. A SEIR-SEIR model in this study is constructed by applying the vaccination program as a parameter. In addition to performing more complete analytical results, we also consider control strategies to understand the effect of the vaccination program.

This paper is organized as follows. In Section 2, we construct a host-vector model of monkeypox transmission. After showing the invariant positivity of the solution, the equilibrium points are determined and its existence conditions investigated. Next, the basic reproduction number is obtained and we consider the existence of equilibrium points in terms of the basic reproduction number. In Section 4, the stability of the equilibrium points is discussed. After that, we introduce control strategies in order to eradicate monkeypox. In Section 5, we perform numerical simulations to provide a complete understanding of monkeypox transmission and to analyze the role of some parameters in the dynamics. Finally, at the end of this paper we give a brief summary.

Model formulation

In the present study, we propose a mathematical model of monkeypox transmission by modifying the model in [Bankuru et al., 2020] and [Peter et al., 2022]. Here, rodent is considered as the primary reservoir host. In this study, we preserve the recovered compartment of rodent to produce a better understanding of monkeypox transmission and put the vaccination program as a parameter since the efficiency of the monkeypox vaccine is quite high so that the susceptible human with vaccination is assumed to be immune [CDC.gov]. In general, the human population (denoted by h) is divided into four compartments, i.e., susceptible humans S_h, exposed humans E_h, infected humans I_h and recovered humans R_h. Furthermore, the rodent population (denoted by r) is also subdivided into the same compartments as human, i.e., susceptible rodents S_r, exposed rodents E_r, infected rodents I_r and

recovered rodents R_r. Let N_h and N_r denote the human and rodent populations size. We assume that population size of humans and rodents remains constant.

　　　Human and rodent populations increase due to the recruitment of humans and rodents at rates Λ_h and Λ_r, respectively. The susceptible human becomes exposed after contact either with an infected human or with an infected rodent at rates β_h and β_{rh}, respectively. Thus, the infection rate β_h is defined as a product of the effective contact rate and the probability of a human being infected by monkeypox after contact with an infected human. This is also analogous to β_r. In addition, the infection rate β_{rh} is defined as a product of the effective contact rate of humans with the probability of a human being infected with monkeypox per contact with an infected rodent. After the incubation period, exposed humans and rodents become infected humans and rodents with the rate φ_h and φ_r, respectively. Each of them may recover and move to R_h (or R_r) compartment with the rate γ_h (or γ_r). Natural death may occur either to humans or to rodents so they are assumed to die due to natural causes at rates μ_h and μ_r, respectively. Since we consider the vaccination, the vaccinated human will move to R_h compartment at a rate α. For brevity, the transition of humans and rodents from one to other compartments as stated above is illustrated in the schematic diagram in Figure 1.
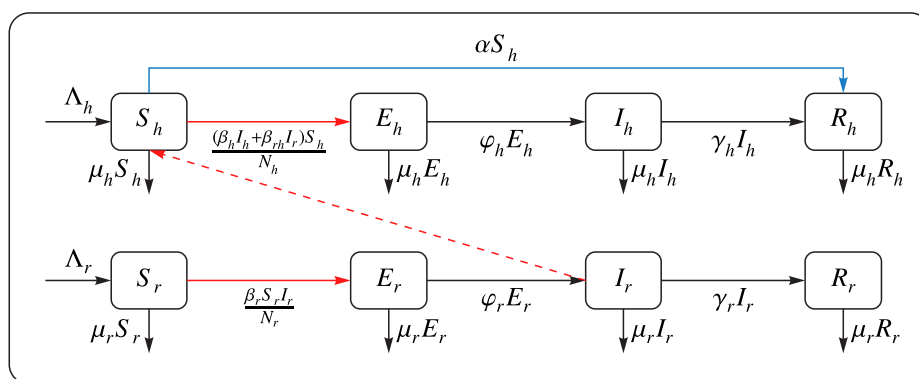

Figure 1. Diagram transmission of monkeypox considering vaccinated people

　　　The schematic diagram is then translated into a mathematical model in the form of differential equations as in the system (1) which is equipped with nonnegative parameters and initial conditions, namely, $S_h(0) \geqslant 0$, $E_h(0) \geqslant 0$, $I_h(0) \geqslant 0$, $R_h(0) \geqslant 0$, $S_r(0) \geqslant 0$, $E_r(0) \geqslant 0$, $I_r(0) \geqslant 0$, and $R_r(0) \geqslant 0$.

$$
\begin{aligned}
\frac{dS_h}{dt} &= \Lambda_h - \frac{(\beta_h I_h + \beta_{rh} I_r)S_h}{N_h} - \alpha S_h - \mu_h S_h, \\
\frac{dE_h}{dt} &= \frac{(\beta_h I_h + \beta_{rh} I_r)S_h}{N_h} - \varphi_h E_h - \mu_h E_h, \\
\frac{dI_h}{dt} &= \varphi_h E_h - \gamma_h I_h - \mu_h I_h, \\
\frac{dR_h}{dt} &= \gamma_h I_h + \alpha S_h - \mu_h R_h, \\
\frac{dS_r}{dt} &= \Lambda_r - \frac{\beta_r S_r I_r}{N_r} - \mu_r S_r, \\
\frac{dE_r}{dt} &= \frac{\beta_r S_r I_r}{N_r} - \varphi_r E_r - \mu_r E_r, \\
\frac{dI_r}{dt} &= \varphi_r E_r - \gamma_r I_r - \mu_r I_r, \\
\frac{dR_r}{dt} &= \gamma_r I_r - \mu_r R_r.
\end{aligned}
\tag{1}
$$

Dynamic analysis

Positive invariant

All variables of the system (1) denote the number of population. Then all of them must be nonnegative for time $t \geqslant 0$ when the initial conditions are also nonnegative from the biological point of view. Next, we need to show that the system (1) is well-posed in the biological sense. From the first equation in the system (1), $\frac{dS_h}{dt} \geqslant -(\alpha + \mu_h)S_h$ for nonnegative initial conditions. Therefore,

$$S(t) \geqslant S_h^0 e^{-(\alpha + \mu_h)t} \geqslant 0. \tag{2}$$

Meanwhile, the fifth equation of (1) implies that $\frac{dS_r}{dt} \geqslant -(\alpha + \mu_r)S_r$ for nonnegative initial conditions. Therefore,

$$S_r(t) \geqslant S_r^0 e^{-(\alpha + \mu_r)t} \geqslant 0, \tag{3}$$

Equations (2) and (3) imply that $S_h(t)$ and $S_r(t)$ remain nonnegative for all times $t > 0$. The same results hold for the other variables in human and rodent population.

The summation of all equations in (1) yields a differential equation for the total population $N_h(t) + + N_r(t)$ as follows:

$$\frac{dN_h + dN_r}{dt} = (\Lambda_h + \Lambda_r) - \mu_h N_h - \mu_r N_r. \tag{4}$$

Solving equation (4) yields $N_h(t) + N_r(t) = \frac{\Lambda_h}{\mu_h} + \frac{\Lambda_r}{\mu_r} + \left(N_h(0) - \frac{\Lambda_h}{\mu_h}\right)e^{-\mu_h t} + \left(N_r(0) - \frac{\Lambda_r}{\mu_r}\right)e^{-\mu_r t}$, where $N_h(0)$ and $N_r(0)$ are the initial total numbers of each population. As a consequence, $N_h(t) + N_r(t) \to \frac{\Lambda_h}{\mu_h} + \frac{\Lambda_r}{\mu_r}$ as $t \to \infty$. Therefore,

$$\Omega = \left\{(S_h, E_h, I_h, R_h, S_r, E_r, I_r, R_r) \in \mathbb{R}_+^8 : 0 \leqslant N_h + N_r \leqslant \frac{\mu_r \Lambda_h + \mu_h \Lambda_r}{\mu_h \mu_r}\right\} \tag{5}$$

is the feasible domain of (1) and proving the positive invariance and the well-posedness of the system.

Basic reproductive number

In this section, we calculate the disease outbreak threshold, i. e., the basic reproductive number to understand the long-term behavior of the epidemic. This threshold represents the average number of cases of secondary infection due to a single infection in a susceptible population. Here, we use the Next-Generation Matrix (NGM) method to calculate $\mathcal{R}_0$.

First of all, to apply the NGM method, we calculate the disease-free equilibrium point of the system (1), which is given by

$$X_0 = \left(S_h^0, E_h^0, I_h^0, R_h^0, S_r^0, E_r^0, I_r^0, R_r^0\right) = \left(\frac{A_h}{\alpha + \mu_h}, 0, 0, \frac{\alpha \Lambda_h}{(\alpha + \mu_h)\mu_h}, \frac{\Lambda_r}{\mu_r}, 0, 0, 0\right). \tag{6}$$

Then, we compute the linearization matrix of four infection compartments of the system (1), namely, E_h, I_h, E_r, and I_r compartments. The evaluation of this matrix at point X_0 is denoted by J matrix, which is obtained as follows:

$$J = \begin{pmatrix} -\varphi_h - \mu_h & \frac{\mu_h \beta_h}{\alpha + \mu_h} & 0 & \frac{\mu_h \beta_{rh}}{\alpha + \mu_h} \\ \varphi_h & -\gamma_h - \mu_h & 0 & 0 \\ 0 & 0 & -\varphi_r - \mu_r & \beta_r \\ 0 & 0 & \varphi_r & -\gamma_r - \mu_r \end{pmatrix}. \tag{7}$$

The Jacobian J can be expressed as $J = F - V$ [Van den Driessche, Watmough, 2002], with

$$F = \begin{pmatrix} 0 & \frac{\mu_h \beta_h}{\alpha + \mu_h} & 0 & \frac{\mu_h \beta_{rh}}{\alpha + \mu_h} \\ 0 & 0 & 0 & 0 \\ 0 & 0 & 0 & \beta_r \\ 0 & 0 & 0 & 0 \end{pmatrix} \quad \text{and} \quad V = \begin{pmatrix} \varphi_h + \mu_h & 0 & 0 & 0 \\ -\varphi_h & \gamma_h + \mu_h & 0 & 0 \\ 0 & 0 & \varphi_r + \mu_r & 0 \\ 0 & 0 & -\varphi_r & \gamma_r + \mu_r \end{pmatrix}. \tag{8}$$

Finally, we can derive the basic reproduction number equation from the spectral radius of the Next-Generation Matrix as follows [Van den Driessche, Watmough, 2002; Van den Driessche, Watmough, 2008; Diekmann, Heesterbeek, Roberts, 2010]:

$$\mathcal{R}_0 = \rho(\mathbf{NGM}) = \rho\left(FV^{-1}\right),$$
$$\mathcal{R}_0 = \max\{\mathcal{R}_{0h}, \mathcal{R}_{0r}\}, \tag{9}$$

where

$$\mathcal{R}_{0h} = \frac{\beta_h \mu_h \varphi_h}{(\varphi_h + \mu_h)(\gamma_h + \mu_h)(\alpha + \mu_h)} \quad \text{and} \quad \mathcal{R}_{0r} = \frac{\beta_r \varphi_r}{(\varphi_r + \mu_r)(\gamma_r + \mu_r)}. \tag{10}$$

Disease-free equilibrium

Theorem 1. *Disease-free equilibrium, X_0, is locally asymptotically stable if $\mathcal{R}_{0h} < 1$ and $\mathcal{R}_{0r} < 1$, and X_0 is unstable under other conditions.*

Proof. The local stability of X_0 is checked from the eigenvalues of the Jacobian system (1) which is evaluated at point X_0, namely $\mathcal{J}(X_0)$. The eigenvalues of $\mathcal{J}(X_0)$ are $-\mu_h$, $-\mu_r$ (multiplicity 2), $-(\alpha + \mu_h)$ and the roots of polynomials

$$(\alpha + \mu_h)\left[\lambda^2 + (\varphi_h + 2\mu_h + \gamma_h)\lambda + (\varphi_h + \mu_h)(\gamma_h + \mu_h)(1 - \mathcal{R}_{0h}\right] = 0 \tag{11}$$

and

$$\lambda^2 + (\gamma_r + 2\mu_r + \varphi_r)\lambda + (\varphi_r + \mu_r)(\mu_r + \gamma_r)(1 - \mathcal{R}_{0r}) = 0. \tag{12}$$

The roots of polynomial (11) are negative if $\mathcal{R}_{0h} < 1$. Moreover, the roots of polynomial (12) are negative if $\mathcal{R}_{0r} < 1$. Therefore, all eigenvalues of $\mathcal{J}(X_0)$ are negative under the condition $\mathcal{R}_{0h} < 1$ and $\mathcal{R}_{0r} < 1$. So, it can be concluded that X_0 is locally asymptotically stable if $\mathcal{R}_{0h} < 1$ and $\mathcal{R}_{0h} > 1$, and X_0 is unstable for other conditions. □

Boundary equilibrium

The second equilibrium of the system (1) is the boundary equilbirium or semi endemic equilibrium, which is denoted by X_1. At this equilibrium point, there is no disease in the rodent population. The boundary equilibrium is obtained as follows:

$$X_1 = \left(S_h^*, E_h^*, I_h^*, R_h^*, S_r^*, 0, 0, 0\right) \tag{13}$$

with

$$S_h^* = \frac{\Lambda_h}{(\alpha + \mu_h)\mathcal{R}_{0h}}, \quad E_h^* = \frac{(\mathcal{R}_{0h} - 1)\Lambda_h}{(\varphi_h + \mu_h)\mathcal{R}_{0h}}, \quad I_h^* = \frac{(\alpha + \mu_h)(\mathcal{R}_{0h} - 1)\Lambda_h}{\mu_h \beta_h},$$

$$R_h^* = \frac{\Lambda_h \gamma_h (\alpha + \mu_h)(\mathcal{R}_{0h} - 1)}{\mu_h^2 \beta_h} + \frac{\Lambda_h \alpha (\varphi_h + \mu_h)(\gamma_h + \mu_h)}{\beta_h \mu_h^2 \varphi_h}, \quad S_r^* = \frac{\Lambda_h}{\mu_r}.$$

So, it can easily be said that the point X_1 exists if $\mathcal{R}_{0h} > 1$.

Theorem 2. *If $\mathcal{R}_{0h} > 1$ and $\mathcal{R}_{0r} < 1$, the boundary equilibrium, X_1, is locally asymptotically stable and for other conditions X_1 is unstable.*

Proof. The local stability of point X_1 is seen from the eigenvalues of the Jacobian system (1) which are evaluated at this point. The eigenvalues of $\mathcal{J}(X_1)$ are $-\mu_h$, $-\mu_r$ (multiplicity 2), and the roots of polynomials

$$\lambda^2 + (\gamma_r + 2\mu_r + \varphi_r)\lambda + (\varphi_r + \mu_r)(\mu_r + \gamma_r)(1 - \mathcal{R}_{0r}) = 0 \tag{14}$$

and

$$a_3\lambda^3 + a_2\lambda^2 + a_1\lambda + a_0 = 0 \tag{15}$$

with

$$\begin{aligned}
a_3 &= (\varphi_h + \mu_h)(\gamma_h + \mu_h), \\
a_2 &= \beta_h\mu_h\varphi_h + (\varphi_h + \mu_h)(\gamma_h + \mu_h)(\varphi_h + 2\mu_h + \gamma_h), \\
a_1 &= \beta_h\mu_h\varphi_h(\varphi_h + 2\mu_h + \gamma_h), \\
a_0 &= (\varphi_h + \mu_h)^2(\gamma_h + \mu_h)^2(\alpha + \mu_h)(\mathcal{R}_{0h} - 1).
\end{aligned} \tag{16}$$

All roots of polynomial (14) are negative if $\mathcal{R}_{0r} < 1$. Whereas, if $\mathcal{R}_{0h} > 1$ then all coefficients of polynomial (15) are positive, $a_0, a_1, a_2, a_3 > 0$. Further, it can be shown that $a_1 a_2 > a_0 a_3$. So, according to the Routh–Hurwitz criteria, all roots of polynomial (15) are negative. Therefore, we can conclude that endemic equilibrium is locally asymptotically stable if $\mathcal{R}_{0r} < 1$ and $\mathcal{R}_{0h} > 1$ and unstable for other conditions. □

Endemic equilibrium

In addition to the disease-free equilibrium point and the boundary equilibrium point, the system (1) has another equilibrium point, namely, the endemic equilibrium point or interior point, which is obtained as:

$$X_2 = \left(S_h^{**}, E_h^{**}, I_h^{**}, R_h^{**}, S_r^{**}, E_r^{**}, I_r^{**}, R_r^{**}\right), \tag{17}$$

with

$$S_h^{**} = \frac{\Delta_1^2\beta_r I_h^{**2}}{\Delta_2}, \quad E_h^{**} = \frac{\gamma_h + \mu_h}{\varphi_h}I_h^{**}, \quad \Delta_1 = (\varphi_h + \mu_h)(\gamma_h + \mu_h),$$

$$\Delta_2 = \varphi_h\left((\mathcal{R}_{0h} - 1)(\varphi_h + \mu_h)(\gamma_h + \mu_h)(\alpha + \mu_h)\beta_r I_h^{**} + \Lambda_r(\mathcal{R}_{0r} - 1)\beta_{rh}\mu_h\varphi_h\right),$$

$$R_h^{**} = \frac{(\gamma_h\varphi_h(\alpha + \mu_h)(\mathcal{R}_{0h} - 1) + \alpha\Delta_1)\Delta_1\beta_r I_h^{**2} + A_r(\mathcal{R}_{0r} - 1)\beta_{rh}\gamma_h\mu_h\varphi_h^2 I_h^{**}}{\Delta_2\mu_h},$$

$$S_r^{**} = \frac{\Lambda_r(\varphi_r + \mu_r)(\gamma_r + \mu_r)}{\beta_r\varphi_r\mu_r}, \quad E_r^{**} = \frac{\Lambda_r(\gamma_r + \mu_r)(\mathcal{R}_{0r} - 1)}{\beta_r\varphi_r}, \quad I_r^{**} = \frac{\Lambda_r(\mathcal{R}_{0r} - 1)}{\beta_r},$$

$$R_r^{**} = \frac{\Lambda_r(\mathcal{R}_{0r} - 1)\gamma_r}{\beta_r\mu_r}.$$

From the equation above, it is easy to conclude that rodent compartments will exist if $\mathcal{R}_{0r} > 1$. Next, we consider I_h^{**} which is implicitly defined by

$$f(I_h^{**}) = b_2\left(I_h^{**}\right)^2 + b_1 I_h^{**} + b_0, \tag{18}$$

where

$$\begin{aligned}
b_2 &= (\varphi_h + \mu_h)(\gamma_h + \mu_h)\beta_h\mu_h, \\
b_1 &= (\varphi_h + \mu_h)(\gamma_h + \mu_h)\frac{\beta_{rh}\mu_h\Lambda_r(\mathcal{R}_{0r} - 1) + \beta_r\Lambda_h(\alpha + \mu_h)(1 - \mathcal{R}_{0h})}{\beta_r}, \\
b_0 &= -\frac{\Lambda_h\Lambda_r(\mathcal{R}_{0r} - 1)\beta_{rh}\mu_h\varphi_h}{\beta_r}.
\end{aligned}$$

According to Descartes' criterion, the polynomial $f\left(I_h^{**}\right)$ has one positive root ($I_h^{**} > 0$) since the sign of the coefficients of polynomial $f\left(I_h^{**}\right)$ changes once, that is, $b_2 > 0$ and $b_0 < 0$ when $\mathcal{R}_{0r} > 1$. Furthermore, assuming $I_h^{**} > 0$, all elements of X_2 in Equation (17) will be positive if

$$\mathcal{R}_{0h} > 1 - \frac{A_r \beta_{rh} \mu_h \varphi_h (\mathcal{R}_{0r} - 1)}{I_h^{**} \beta_r (\varphi_h + \mu_h)(\gamma_h + \mu_h)(\alpha + \mu_h)}. \tag{19}$$

Thus, X_2 is guaranteed to exist when $\mathcal{R}_{0r} > 1$ and condition (19) satisfied.

Forward bifurcation in $\mathcal{R}_{0r} = 1$

Since the point X_2 is obtained implicitly, the stability of the point X_2 cannot be determined by a linearized matrix. Therefore, the stability of X_2 will be investigated by applying the central manifold theorem [Castillo-Chavez, Song, 2004] written in Theorem 3.

Theorem 3 (see [Castillo-Chavez, Song, 2004]). *Consider the general system of ordinary differential equations with a parameter ϕ as follows*:

$$\frac{dx}{dt} = f(x, \phi), \ f : \mathbb{R}^n \to \mathbb{R} \quad and \quad f \in C^2\left(\mathbb{R}^n \times \mathbb{R}\right). \tag{20}$$

Without loss of generality, it is assumed that $x = 0$ is an equilibrium for the system (20) *for all values of the parameter ϕ, that is,*

$$f(0, \phi) \equiv 0 \quad for \ all \ \phi. \tag{21}$$

Assume

A1: $\mathbf{A} = D_x f(0, 0) = \left(\frac{\partial f_i}{\partial x_j}(0, 0)\right)$ *is the linearization matrix of the system* (20) *around the equilibrium $x = 0$ with ϕ evaluated at 0. Zero is a simple eigenvalue of $\mathbf{A}$ and all other eigenvalues of $\mathbf{A}$ have negative real parts;*

A2: *Matrix $\mathbf{A}$ has a nonnegative right eigenvector $\mathbf{w}$ and a left eigenvector $\mathbf{v}$ corresponding to the zero eigenvalue.*

Let f_k be the kth component of f and

$$a = \sum_{k,i,j=1}^{n} v_k w_i w_j \frac{\partial^2 f_k}{\partial x_i \, \partial x_j}(0, 0) \quad and \quad b = \sum_{k,i=1}^{n} v_k w_i \frac{\partial^2 f_k}{\partial x_i \, \partial \phi}(0, 0). \tag{22}$$

The local dynamics of the system (20) *around $x = 0$ are totally determined by a and b.*

1. *$a > 0$, $b > 0$. When $\phi < 0$ with $|\phi| \ll 1$, $x = 0$ is locally asymptotically stable, and there exists a positive unstable equilibrium; when $0 < \phi \ll 1$, $x = 0$ is unstable and there exists a negative and locally asymptotically stable equilibrium.*

2. *$a < 0$, $b > 0$. When ϕ changes from negative to positive, $x = 0$ changes its stability from stable to unstable. Hence, a negative unstable equilibrium becomes positive and locally asymptotically stable.*

From Theorem 3, it can be concluded that if condition (1) is satisfied, then a backward bifurcation occurs, whereas if condition (2) is met, then a forward bifurcation occurs.

The system (1) can be rewritten as

$$\frac{dX(t)}{dt} = \mathcal{F}(X(t)) = (f_1, f_2, \ldots, f_8)^T, \tag{23}$$

with $X(t) = (x_1, x_2, \ldots, x_8)^T = (S_h, E_h, I_h, R_h, S_r, E_r, I_r, R_r)^T$. Now, we investigate the existence of a bifurcation around $\mathcal{R}_{0r} = 1$ when $\mathcal{R}_{0h} > 1$, which is equivalent to $\beta_h > \frac{(\varphi_h + \mu_h)(\gamma_h + \mu_h)(\alpha + \mu_h)}{\mu_h \varphi_h}$ with β_r as the bifurcation parameter. To apply the theorem, we first check the eigenvalues of the Jacobian matrix $\mathcal{J}\left(X_1, \beta_r^*\right)$. The characteristic polynomial of $\mathcal{J}\left(X_1, \beta_r^*\right)$ is

$$
\begin{aligned}
P(\lambda) &= \lambda(\lambda + \mu_r)^2(\lambda + \mu_r)(\lambda + \gamma_r + 2\mu_r + \varphi_r)\left(a_3\lambda^3 + a_2\lambda^2 + a_1\lambda + a_0\right)(\varphi_h + \mu_h)(\gamma_h + \mu_h), \\
a_3 &= (\varphi_h + \mu_h)(\gamma_h + \mu_h), \\
a_2 &= \beta_h\mu_h\varphi_h + (\varphi_h + \mu_h)(\gamma_h + \mu_h)(\varphi_h + 2\mu_h + \gamma_h), \\
a_1 &= \beta_h\mu_h\varphi_h(\varphi_h + 2\mu_h + \gamma_h), \\
a_0 &= (\varphi_h + \mu_h)^2(\gamma_h + \mu_h)^2(\alpha + \mu_h)(\mathcal{R}_{0h} - 1).
\end{aligned}
\tag{24}
$$

For $\mathcal{R}_{0h} > 1$, the polynomial $a_3\lambda^3 + a_2\lambda^2 + a_1\lambda + a_0$ has three negative roots (as evidenced by Equation (15)). Thus, it is clear that the polynomial $P(\lambda)$ (24) has one "0" eigenvalue and all other eigenvalues have negative real parts. Then, we calculate the right eigenvector $\mathbf{w}$ with $\mathcal{J}(X_1, \beta_r^*) \cdot \mathbf{w} = 0$ and the left eigenvector $\mathbf{v}$ with $\mathbf{v} \cdot \mathcal{J}\left(X_1, \beta_r^*\right) = 0$, which correspond to a zero eigenvalue. We obtain the right eigenvector as

$$
\mathbf{w} = \left[-\frac{\eta_3\eta_2}{\eta_1\varphi_h}, \frac{\eta_3}{\varphi_h}, 1, \frac{\alpha - \gamma_h}{\eta_1} - \frac{\alpha\eta_3}{\varphi_h\eta_1}, \frac{\beta_h\eta_4\eta_5(1 - \mathcal{R}_{0h})}{\beta_{rh}\mu_r\varphi_h}, \frac{\beta_h\eta_5(\mathcal{R}_{0h} - 1)}{\beta_{rh}\varphi_r}, \frac{\beta_h(\mathcal{R}_{0h} - 1)}{\beta_{rh}}, \frac{\beta_h(\mathcal{R}_{0h} - 1)\varphi_r}{\beta_{rh}\mu_r} \right],
\tag{25}
$$

where

$$
\eta_1 = \alpha + \mu_h, \quad \eta_2 = \varphi_h + \mu_h, \quad \eta_3 = \gamma_h + \mu_h, \quad \eta_4 = \varphi_r + \mu_r, \quad \eta_5 = \mu_r + \gamma_r.
\tag{26}
$$

And the left eigenvector satisfies $\mathbf{v} \cdot \mathbf{w} = 1$:

$$
\mathbf{v} = \left[0, 0, 0, 0, 0, \frac{\beta_{rh}\varphi_r}{\beta_r(\mathcal{R}_{0h} - 1)(\eta_4 + \eta_5)}, \frac{\beta_{rh}\eta_4}{\beta_r(\mathcal{R}_{0h} - 1)(\eta_4 + \eta_5)} \right].
\tag{27}
$$

Finally, we can calculate the coefficients a and b as

$$
a = \sum_{k,i,j=1}^{n} v_k w_i w_j \frac{\partial^2 f_k}{\partial x_i \partial x_j}\left(X_1, \beta_r^*\right) = -2\frac{\beta_h\beta_r(\mathcal{R}_{0h} - 1)}{\beta_{rh}\Lambda_r(\eta_4 + \eta_5)}
\tag{28}
$$

and

$$
b = \sum_{k,i=1}^{n} v_k w_i \frac{\partial^2 f_k}{\partial x_i \partial \phi}\left(X_1, \beta_r^*\right) = \frac{\varphi_r}{\eta_4 + \eta_5}.
\tag{29}
$$

Under the conditions applied to the assumption $\mathcal{R}_{0h} > 1$, we get $a < 0$ and $b > 0$. It can be concluded that a forward bifurcation occurs at $\mathcal{R}_{0r} = 1$. For $\mathcal{R}_{0r} < 1$, X_1 exists and is stable, then for $\mathcal{R}_{0r} > 1$, X_1 becomes unstable and X_2 exists and is stable. An illustration of the change in stability of these two points is shown in Figure 6.

Theorem 4.   *Endemic equilibrium, X_2, is locally asymptotically stable if $\mathcal{R}_{0h} > 1$ and $\mathcal{R}_{0r} > 1$, and X_2 is unstable under other conditions.*

Optimal control

In this study, we have considered a control variable α used to vaccinate the susceptible population in humans. The optimal control problem is constructed for minimizing the exposed and infected

individuals as well as the cost of implementing the vaccination. Thus, the objective functional is defined as follows:

$$J(\alpha) = \frac{1}{2} \int_0^{t_f} v_1 E_h^2(t) + v_2 I_h^2(t) + w\alpha^2(t) \, dt, \tag{30}$$

where $v_i > 0$, for $i = 1, 2$, and $w > 0$ are the weighting parameters for the state variable and the control variable (α), respectively. The t_f represents the time final to control monkeypox. Here, we apply Pontryagin's minimum principle to solve the optimal control problem. The Hamiltonian function is given by

$$H = \frac{1}{2}\left(v_1 E_h^2(t) + v_2 I_h^2(t) + w\alpha^2(t)\right) + \sum_{j=1}^8 \lambda_j \frac{dX_j}{dt}, \tag{31}$$

where $X = (S_h, E_h, I_h, R_h, S_r, E_r, I_r, R_r)^T$. Here, λ_j denotes the associated co-state for the state X_j, which is the solution of the co-state system

$$\frac{d\lambda_j}{dt} = -\frac{\partial H}{\partial X_j}. \tag{32}$$

Furthermore, we determine the optimal control α^* that minimizes the Hamiltonian function, i.e., α satisfying the condition $\frac{dH}{d\alpha} = 0$. Thus, we obtain

$$\alpha^*(t) = \min\left\{1, \max\left[0, \frac{S_h(\lambda_1 - \lambda_4)}{w}\right]\right\}. \tag{33}$$

Numerical simulation

In this section, we perform a numerical simulation based on the results of the dynamic analysis of the model obtained in the previous section. The numerical simulation is carried out using the parameter values in Table 1.

Table 1. Description of parameters

Parameter	Value	Description	Source
Λ_h	$\mu_h \cdot N_h$	Recruitment humans rate	[CIA.gov]
Λ_r	$\mu_h \cdot N_r$	Recruitment rodents rate	[Hayssen, 2008]
μ_h	$\frac{1}{70 \cdot 365}$	Humans death rate	[The world bank]
μ_r	$\frac{1}{2 \cdot 365}$	Rodents death rate	[Hayssen, 2008]
$\frac{1}{\gamma_h}$	28	Human latent period	[Nolen et al., 2016]
$\frac{1}{\gamma_r}$	28	Rodent latent period	[WHO]
$\frac{1}{\varphi_h}$	14	Human infection period	[Di Giulio, Eckburg, 2004]
$\frac{1}{\varphi_r}$	14	Rodent infection period	[Di Giulio, Eckburg, 2004]
α	[0, 1]	Proportion of vaccination program rate	assumed
β_h	[0, 1]	Infection rate of S_h form I_h	assumed
β_r	[0, 1]	Infection rate of S_r form I_r	assumed
β_{rh}	[0, 1]	Infection rate of S_h form I_r	assumed

Sensitivity $\mathcal{R}_0$

In this subsection, we study the effect of each parameter on $\mathcal{R}_0$ through the level set and sensitivity index. Figure 2, *a* shows the contour plot of $\mathcal{R}_{0h}$ in the plane-$\alpha\beta_h$ and Figure 2, *b* shows the plot of $\mathcal{R}_{0r}$ versus β_r. From the equation $\mathcal{R}_{0h}$, we pay attention to two parameters that play an important role in transmission, i. e., α and β_h. From Figure 2, *a*, it can be observed that the greater interactions number between infected humans and susceptible humans will increase the number of the incidences of monkeypox which is indicated by the increasing of $\mathcal{R}_{0h}$ value. However, this level set of $\mathcal{R}_{0h}$ implies that the high value of $\mathcal{R}_{0h}$ can be suppressed by increasing the value of α even though β_h stays in a certain high value. It means that if the infection rate of susceptible human by infected human cannot be decreased, then the spread of monkeypox can be eradicated by increasing the vaccination rate. These results show that the vaccination program is able to prevent the monkeypox transmission. Meanwhile, Figure 2, *b* shows that the increase in β_r also increases the value of $\mathcal{R}_{0r}$. This is acceptable, because the higher the interaction between infected and susceptible rodents, the higher the number of cases of infection.
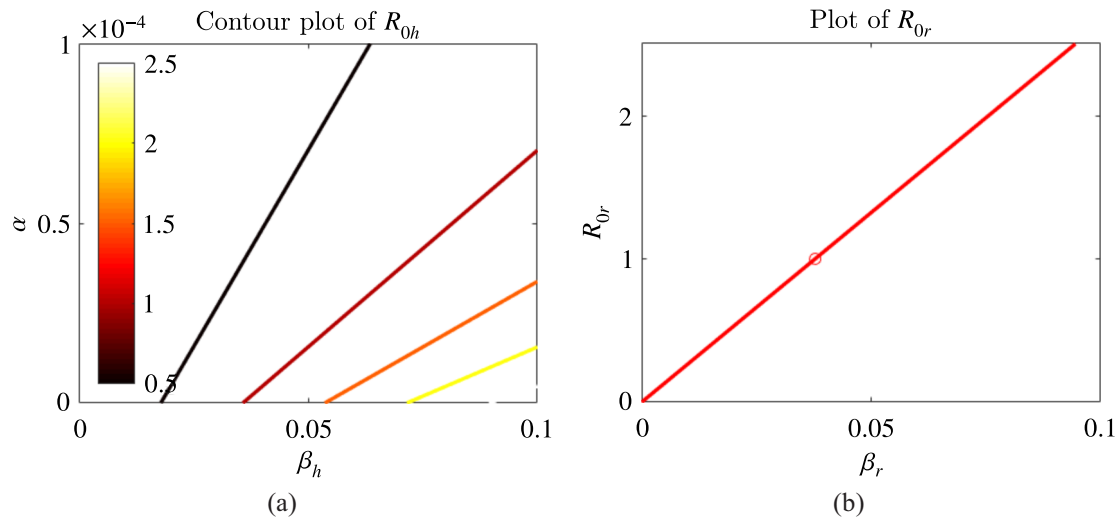

Figure 2. (a) Contour plot of $\mathcal{R}_{0h}$ in the plane-$\beta_h\alpha$ and (b) plot of $\mathcal{R}_{0r}$ versus β_r

We analyzed the sensitivity of $\mathcal{R}_0$ to model parameters using a normalized forward sensitivity index as defined in [Chitnis, Hyman, Cushing, 2008]. In particular, the forward sensitivity index of the normalized variable u, which depends on the parameter p, is defined as

$$\Upsilon_p^u = \frac{\partial u}{\partial p} \times \frac{p}{u}. \tag{34}$$

Table 2 shows the sensitivity index of $\mathcal{R}_0$ calculated on $\mathcal{R}_{0h}$ and $\mathcal{R}_{0r}$. From Table 2 it can be seen that Λ_h parameter has no effect on $\mathcal{R}_{0h}$ and Λ_r parameter has no effect on $\mathcal{R}_{0r}$. For parameter sets applied with $\alpha = 0.00001$, $\mathcal{R}_{0h} = \mathcal{R}_{0r} = 3$, then $\mathcal{R}_{0h}$ is most affected by the β_h parameter, then φ_h, α, μ_h and γ_h. Every 10 % increase in value of β_h, then $\mathcal{R}_{0h}$ will increase by 10 %. Conversely, 10 % increases α, then $\mathcal{R}_{0h}$ will decrease by 7.1 %. Meanwhile, $\mathcal{R}_{0r}$ is most affected by β_r, then φ_r, μ_r, and γ_r. An increase in β_r by 10 % will increase $\mathcal{R}_{0r}$ by 10 %. This table also shows that infection from rodents to humans (β_{rh}) does not directly affect $\mathcal{R}_0$. It can be concluded that the most influential factor in controlling the increasing of infected number is the infected rate in both human and rodent population.

The equation of $\mathcal{R}_0$ (10) is independent of β_{rh}, so from this we do not see the effect of β_{rh} on $\mathcal{R}_0$. However, given that β_{rh} represents the infection rate from infected rodents to susceptible humans, it is

Table 2. Sensitivity index of $\mathcal{R}_0$ corresponds to the value of the parameter in Table 1 and $\alpha = 0.00001$ for $\mathcal{R}_{0h} = 3$ and $\mathcal{R}_{0r} = 3$

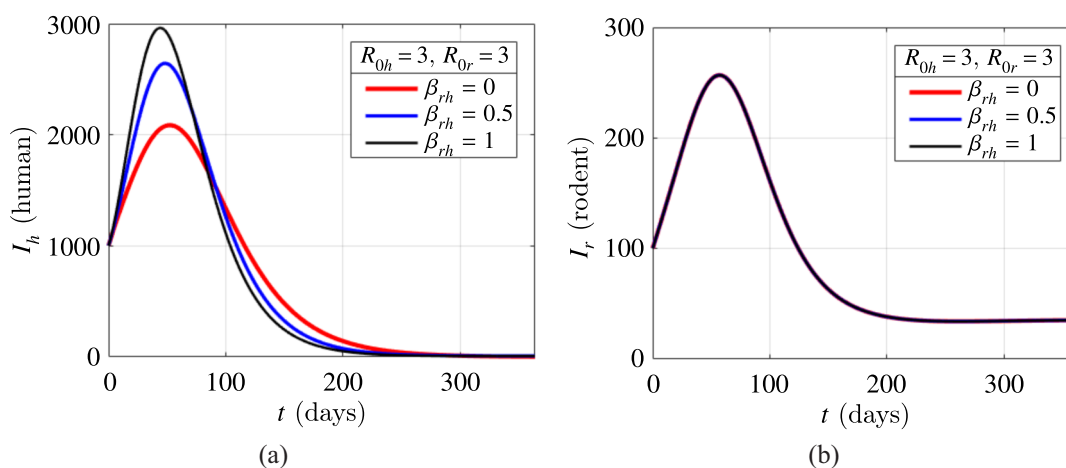|	Parameter (p)	Sensitivity index $\left(\Upsilon_p^{\mathcal{R}_{0h}}\right)$			Parameter (p)	Sensitivity index $\left(\Upsilon_p^{\mathcal{R}_{0r}}\right)$
1.	Λ_h	0		1.	Λ_h	0
2.	Λ_r	0		2.	Λ_r	0
3.	μ_h	0.71706		3.	μ_h	0
4.	μ_r	0		4.	μ_r	−0.05575
5.	γ_h	0.00054		5.	γ_h	0
6.	γ_r	0		6.	γ_r	0.018817
7.	φ_h	−0.99890		7.	φ_h	0
8.	φ_r	0		8.	φ_r	−0.96306
9.	α	−0.71870		9.	α	0
10.	β_h	1		10.	β_h	0
11.	β_r	0		11.	β_r	1
12.	β_{rh}	0		12.	β_{rh}	0

Figure 3. Solutions of I_h and I_r from System (1) with variations in β_{rh} values

odd that a change in the value of β_{rh} would not affect the increase in the number of infected humans. We simulate the system (1) with variations in the value of β_{rh} for constant $\mathcal{R}_{0h}$ and $\mathcal{R}_{0r}$, which is shown in Figure 3. In Figure 3, it can be seen that changes in β_{rh} values affect the number of infections in humans, where the higher the β_{rh} value, the higher the peak of infection humans. However, the changes in β_{rh} values had no effect on the rodent compartments.

The stability of equilibria

Based on the analysis of the stability of the equilibrium points, the plane-$\mathcal{R}_{0h}\mathcal{R}_{0r}$ is divided into four parts of the stability region as shown in Figure 4. The region of existence and stability of the equilibrium points is as follows: (1) A_1: X_0 exists and is stable, (2) A_2: X_0 exists and is unstable, and X_1 exists and is stable, (3) A_3: X_0 and X_1 exists and is unstable, and X_2 exists and is stable, and (4) A_4: X_0 exists and is unstable. This result is acceptable, in the area A_2, under the conditions $\mathcal{R}_{0h} > 1$, while $\mathcal{R}_{0r} < 1$, the disease in the rodent population will be extinct, because there is no transmission from humans to rodents, but the disease in the human population will still exist due

to human-to-human transmission. Furthermore, in the area A_3, where $\mathcal{R}_0 > 1$, the disease will exist and become endemic in human and rodent populations.
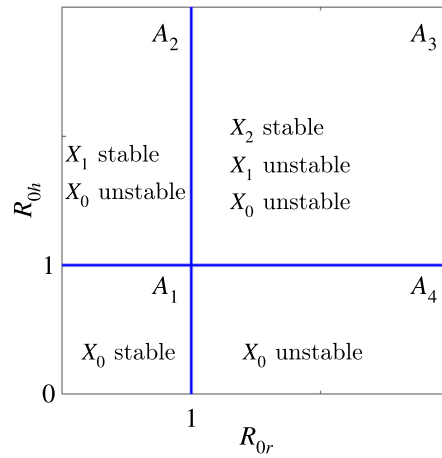

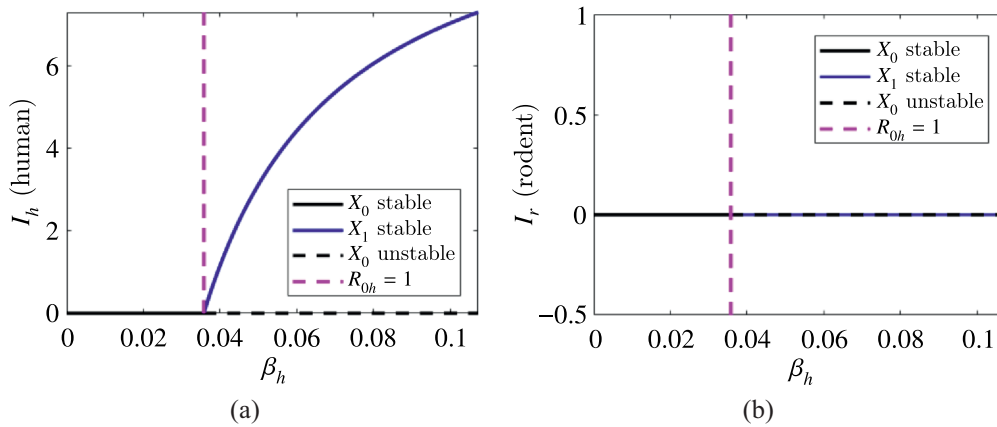Figure 4. Stability area of equilibria in plane-$\mathcal{R}_{0r}\mathcal{R}_{0h}$

Figure 5. Bifurcation diagrams around $\mathcal{R}_{0h} = 1$ for $\mathcal{R}_{0r} < 1$ for (a) I_h versus β_h and (b) I_r versus β_h
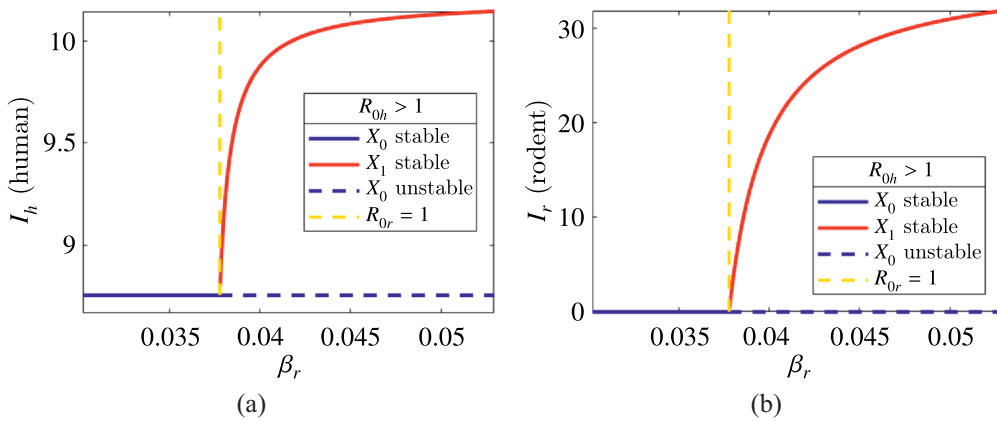

Figure 6. Bifurcation diagrams around $\mathcal{R}_{0r} = 1$ for $\mathcal{R}_{0h} > 1$ for (a) I_h versus β_h and (b) I_r versus β_h

The change of stability and forward bifurcation from points $X_0 - X_1$ and $X_1 - X_2$ is shown in Figure 5 and 6. Figure 5 shows forward bifurcation around $\mathcal{R}_{0h} = 1$ (form A_1 to A_2). Before $\mathcal{R}_{0h} = 1$, X_0 exists and is stable, and after $\mathcal{R}_{0h} = 1$, X_0 becomes unstable and X_1 exists and is stable. This bifurcation diagram corresponds to Theorem 1 and Theorem 2 about the stability of X_0 and X_1. Figure 6 shows a forward bifurcation around $\mathcal{R}_{0r} = 1$ (form A_2 to A_3). Before $\mathcal{R}_{0r} = 1$, X_1 stable, and after $\mathcal{R}_{0r} = 1$, X_1 becomes unstable and X_2 exists and is stable. This simulation is in agreement with the bifurcation analysis carried out in Subsection 2.

Assessment of control strategies: vaccine program

We solve the optimal control problem numerically using the backward-forward sweep method with the Runge–Kutta solver. The state system (1) is solved forward in time using an estimate for the control and co-state variables, and then the co-state system (32) is solved backwards in time [McAsey, Mou, Han, 2012]. We set the initial conditions $S_h(0) = 7.000$, $E_h(0) = 1.000$, $I_h(0) = 1.000$, $R_h(0) = 1.000$, $S_r(0) = 300$, $E_r(0) = 100$, $I_r(0) = 100$, and $R_r(0) = 100$, and the parameter values as shown in Table 1. By selecting the parameters $\beta_r = 0.1134$, $\beta_h = 0.1073$, and $\beta_{rh} = 0.1$, we obtain $R_0 = 3$. Therefore, a control is needed to reduce the number of infected individuals.
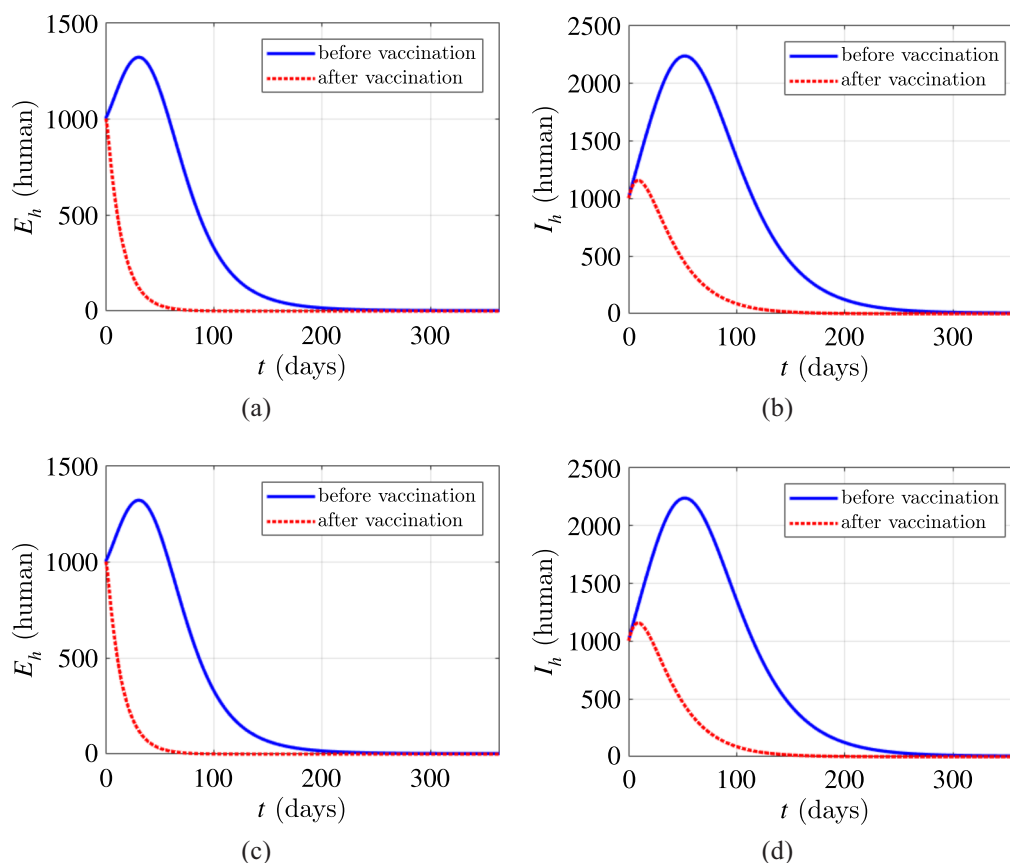

Figure 7. Dynamics of (a) exposed human, (b) infected human, and (c) infected rodent compartments. (d) The optimal vaccination profile of α

Figures 7, *a* and 7, *b* show the dynamics of exposed and infected human compartments, respectively, both with and without vaccination. It can be seen that the vaccination is very effective for reducing the number of infected individuals. Figure 7, *d* represents the optimal vaccination control α^* for 365 days. The optimal vaccination control profile was at the upper bound until time $t = 127.7$ days before decreasing slowly to the lower bound at the end of time.

Conclusion

In this paper, we study the transmission of monkeypox disease through the SEIR-SEIR host-vector model involving vaccination. In this model, there are three ways of infection, i. e., infection from infected humans to susceptible humans, from infected rodents to susceptible humans, and from infected rodents to susceptible rodents. As a disease outbreak threshold, the basic reproduction number is calculated by the next-generation matrix method. From the dynamic analysis of the model, three equilibrium points are obtained according to the existence and stability conditions. They are the disease-free equilibrium point, the boundary or semi-endemic equilibrium point, and the interior or endemic equilibrium point. The endemic equilibrium point cannot be stated explicitly, but its existence conditions can be determined, while the stability is investigated by using the application of the center manifold theorem. From the analysis of the sensitivity index $\mathcal{R}_0$, it is known that infection from infected humans to susceptible humans and infection from infected rodents to susceptible rodents have a direct effect to the increase of $\mathcal{R}_0$. However, the interaction effect from infected rodents to susceptible humans could not be seen from the analysis of $\mathcal{R}_0$ since this parameter does not exist in the expression of $\mathcal{R}_0$. Thus, we carried out a numerical analysis and found that interactions from infected rodents to susceptible humans also resulted in an increase to the number of infected humans. Therefore, it can be concluded that there is also the effect of interaction between infectious rodents and susceptible humans to increase the $\mathcal{R}_0$ indirectly. Furthermore, the vaccination strategy is included in the model as an optimal control problem. The optimal control was obtained by using Pontryagin's maximum principle and solved numerically using the forward-backward sweep method. The simulation results indicate that vaccination is effective to prevent the spread of monkeypox transmission.

References

Alakunle E., Moens U., Nchinda G., Okeke M. I. Monkeypox Virus in Nigeria: infection biology, epidemiology, and evolution // Viruses. — 2020. — Vol. 12, No. 11. — P. 1257.

Bankuru S. V., Kossol S., Hou W., Mahmoudi P., Rychtář J., Taylor D. A game-theoretic model of monkeypox to assess vaccination strategies // PeerJ. — 2020. — Vol. 8. — P. e9272.

BBC News. Monkeypox, two more confirmed cases of viral infection, 2022. — https://www.bbc.com/news/uk-england-london-61449214 (accessed: 2022-10-20).

Bell D. J., Cunningham A. A. Monkeypox: we cannot afford to ignore yet another warning // CABI One Health. — 2022. — No. 2022.

Bhattacharya D., Dhama K., Chakraborty C. Recently spreading human monkeypox virus infection and its transmission during COVID-19 pandemic period: A travelers' prospective // Travel Medicine and Infectious Disease. — 2022. — Vol. 49. — P. 102398.

Bryer J. S., Freeman E. E., Rosenbach M. Monkeypox emerges on a global scale: a historical review and dermatological primer // Journal of the American Academy of Dermatology. — 2022.

Castillo-Chavez C., Song B. Dynamical models of tuberculosis and their applications // Mathematical Biosciences & Engineering. — 2004. — Vol. 1, No. 2. — P. 361.

CDC.gov. Monkeypox vaccination basics. — https://www.cdc.gov/poxvirus/monkeypox/vaccines/vaccine-basics.html (accessed: 2022-12-9).

Chitnis N., Hyman J. M., Cushing J. M. Determining important parameters in the spread of malaria through the sensitivity analysis of a mathematical model // Bulletin of mathematical biology. — 2008. — Vol. 70, No. 5. — P. 1272.

CIA.gov. Birth rate. — https://www.cia.gov/the-world-factbook/field/birth-rate/ (accessed: 2022-12-9).

Diekmann O., Heesterbeek J., Roberts M. G. The construction of next-generation matrices for compartmental epidemic models // Journal of the royal society interface. — 2010. — Vol. 7, No. 47. — P. 873–885.

Di Giulio D. B., Eckburg P. B. SHuman monkeypox: an emerging zoonosis // The Lancet infectious diseases. — 2004. — Vol. 4, No. 1. — P. 15–25.

Gov.UK. Monkeypox outbreak: epidemiological overview, 20 September 2022. — https://www.gov.uk/government/publications/monkeypox-outbreak-epidemiological-over-view/monkeypox-outbreak-epidemiological-overview-20-september-2022 (accessed: 2022-10-20).

Guarner J., Johnson B. J., Paddock C. D., Shieh W. J., Goldsmith C. S., Reynolds M. G., Damon I. K., Regnery R. L., Zaki S. R. et al. Monkeypox transmission and pathogenesis in prairie dogs // Emerging infectious diseases. — 2004. — Vol. 10, No. 3. — P. 426.

Hayssen V. Reproductive effort in squirrels: ecological, phylogenetic, allometric, and latitudinal patterns // Journal of Mammalogy — 2008. — Vol. 89, No. 3. — P. 582–606.

Hu B. L. Scalar waves in the Mixmaster Universe. II. Particle creation // Phys. Rev. D. — 1974. — Vol. 9, No. 9. — P. 3263–3281.

Kampf G. Efficacy of biocidal agents and disinfectants against the monkeypox virus and other orthopoxviruses // Journal of Hospital Infection. D. — Elsevier, 2022.

Khaloufi I., Benfatah Y., Laarabi H., Rachik M. A scenario to fight monkeypox using a mathematical model // Commun. Math. Biol. Neurosci. — 2022.

Kumar N., Acharya A., Gendelman H. E., Byrareddy S. N. The 2022 outbreak and the pathobiology of the monkeypox virus // Journal of Autoimmunity. — Elsevier, 2022. — P. 102855.

Lai C. C., Hsu C. K., Yen M. Y., Lee P. I., Ko W. C., Hsueh P. R. Monkeypox: an emerging global threat during the COVID-19 pandemic // Journal of Microbiology, Immunology and Infection. — 2022.

McAsey M., Mou L., Han W. Convergence of the forward-backward sweep method in optimal control // Computational Optimization and Applications. — 2012. — Vol. 53, No. 1. — P. 207–226.

McCollum A. M., Damon I. K. Human monkeypox // Oxford University Press: Clinical infectious diseases. — 2014. — Vol. 58, No. 2. — P. 260–267.

Meo S. A., Jawaid S. A. Human monkeypox: fifty-two years based analysis and updates // Professional Medical Publications: Pakistan Journal of Medical Sciences. — 2022. — Vol. 38, No. 6. — P. 1416.

Murphy H., Ly H. The potential risks posed by inter-and intraspecies transmissions of monkeypox virus // Taylor & Francis: Virulence. — 2022. — Vol. 13, No. 1. — P. 1681–1683.

Nolen L. D., Osadebe L., Katomba J., Likofata J., Mukadi D., Monroe B., Doty J., Hughes C. M., Kabamba J., Malekani J., et al. Extended human-to-human transmission during a monkeypox outbreak in the Democratic Republic of the Congo // Centers for Disease Control and Prevention: Emerging infectious diseases. — 2016. — Vol. 22, No. 6. — P. 1014.

Peter O. J., Kumar S., Kumari N., Oguntolu F. A., Oshinubi K., Musa R. Modeling Earth systems and environment // Springer. — 2022. — Vol. 8, No. 3. — P. 3423–3434.

Pritomanov S. A. Quantum effects in Mixmaster Universe // Phys. Lett. A. — 1985. — Vol. 107, No. 1. — P. 33–35.

Reuters. Monkeypox cases around the world, 2022 // Factbox. — 2022.

Reynolds M. G., Doty J. B., McCollum A. M., Olson V. A., Nakazawa Y. Monkeypox re-emergence in Africa: a call to expand the concept and practice of One Health // Taylor & Francis: Expert review of anti-infective therapy. — 2019. — Vol. 17, No. 2. — P. 129–139.

Ryan M. P., Shepley L. C. Homogeneous relativistic cosmologies. — Princeton: Princeton series in Physics, 1975. — 336 p.

Sah R., Mohanty A., Abdelaal A., Reda A., Rodriguez-Morales A. J., Henao-Martinez A. F. First monkeypox deaths outside Africa: no room for complacency // SAGE Publications Sage UK: London, England: Therapeutic Advances in Infectious Disease. — 2022. — Vol. 9. — P. 20499361221124027.

The world bank. Life expectancy at birth, total (years). — https://data.worldbank.org/indica-tor/SP.DYN.LE00.IN (accessed: 2022-12-9).

Usman S., Ibrahim I. A. Modeling the transmission dynamics of the monkeypox virus infection with treatment and vaccination interventions // Journal of Applied Mathematics and Physics. — 2017. — Vol. 5, No. 12. — P. 23–35.

Van den Driessche P., Watmough J. Reproduction numbers and sub-threshold endemic equilibria for compartmental models of disease transmission // Mathematical biosciences. — 2002. — Vol. 180, No. 1–2. — P. 29–48.

Van den Driessche P., Watmough J. Further notes on the basic reproduction number // Mathematical epidemiology. — Springer, 2008. — P. 159–178.

Velavan T. P., Meyer C. G. Monkeypox 2022 outbreak: an update // Tropical Medicine & International Health. — 2022.

WHO. Monkeypox. — https://www.who.int/news-room/questions-and-answers/item/monkey-pox?gclid=EAIaIQobChMI-eDxneXw-gIVyhErCh1eag5fEAAYASAAEgJxDPD_BwE (accessed: 2022-10-20).